# Adjoint error estimation for residual based discretizations of hyperbolic conservation laws I: linear problems

Stefano d'Angelo, Mario Ricchiuto, Remi Abgrall, Herman Deconinck


# Adjoint error estimation for residual based discretizations of hyperbolic conservation laws I : linear problems

S. D'Angelo, M . Ricchiuto, R. Abgrall, H. Deconinck

RESEARCH REPORT
N° 7613
May 2011
Project-Teams BACCHUS

ISSN 0249-6399 ISRN INRIA/RR--7613--FR+ENG

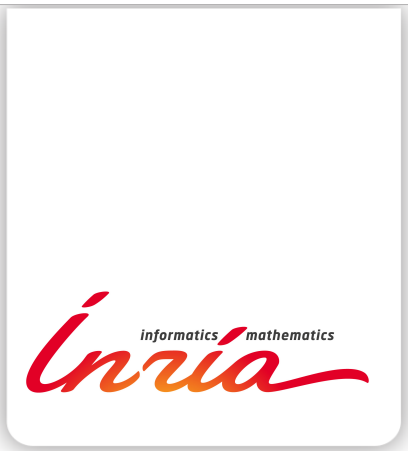


# Adjoint error estimation for residual based discretizations of hyperbolic conservation laws I : linear problems

S. D'Angelo*, M . Ricchiuto†, R. Abgrall‡, H. Deconinck§

Project-Teams BACCHUS

Research Report n° 7613 — May 2011 — 21 pages

**Abstract:** The current work concerns the study and the implementation of a modern algorithm for error estimation in CFD computations. This estimate involves the dealing of the adjoint argument. By solving the adjoint problem, it is possible to obtain important information about the transport of the error towards the quantity of interest. The aim is to apply for the first time this procedure into Petrov-Galerkin (PG) method. Streamline Upwind Petrov-Galerkin, stabilised Residual Distribution and bubble method are involved for the implementation. Scalar linear hyperbolic problems are used as test cases.

**Key-words:** Error Estimation, adjoint problem, Petrov-Galerkin method, Residual Distribution scheme, advection-reaction problem

* Aeronautics and aerospace department, von Karman Institute for Fluid Dynamics, Belgium
† INRIA Bordeaux Sud-Ouest, Equipe BACCHUS
‡ INRIA Bordeaux Sud-Ouest, Equipe BACCHUS
§ Aeronautics and aerospace department, von Karman Institute for Fluid Dynamics, Belgium

**RESEARCH CENTRE**
**BORDEAUX – SUD-OUEST**

351, Cours de la Libération
Bâtiment A 29
33405 Talence Cedex

# Adjoint error estimation for residual based discretizations of hyperbolic conservation laws I : linear problems

**Résumé :** The current work concerns the study and the implementation of a modern algorithm for error estimation in CFD computations. This estimate involves the dealing of the adjoint argument. By solving the adjoint problem, it is possible to obtain important information about the transport of the error towards the quantity of interest. The aim is to apply for the first time this procedure into Petrov-Galerkin (PG) method. Streamline Upwind Petrov-Galerkin, stabilised Residual Distribution and bubble method are involved for the implementation. Scalar linear hyperbolic problems are used as test cases.

**Mots-clés :** Error Estimation, adjoint problem, Petrov-Galerkin method, Residual Distribution scheme, advection-reaction problem

# Contents



# 1 Introduction

Over the last decade, much progress has been made in the area of Error Estimation. This theory provides a way to construct error indicators for CFD computations of PDE's. These error indicators can be used to drive automatic mesh adaptation algorithms. By adapting the mesh, we optimize the mesh spacings or reduce memory usage.
In this field, the *a posteriori* error analysis is one of the most used procedures to compute numerical error indicators. The relevance and generality of this estimation has been powerfully argued in the work of Johnson and his collaborators [1]. The *a posteriori* error bounds resulting from this analysis involve the numerical residual, obtained by inserting the computed solution into the current problem equations; this residual measures the extent to which the numerical approximation to the analytical solution fails to satisfy the current problem. From this study, the *Type II a posteriori* error bounds have been defined.
Becker and Rannacher worked also on this issue and they developed the so-called weighted-residual-based, or *Type I*, *a posteriori* error estimation ([2] and [3]). Here, the error representation formula defines the error in the target functional with the numerical residual, weighted by the solution of an adjoint problem. The key ingredient is this auxiliary problem, involving the formal adjoint of the current partial differential operator. For computing this product, also this adjoint problem will have to be implemented and solved numerically. For solving the adjoint problem, added cost rises. However, it is paid back by important information which helps us to identify where the real source of the error comes from. For example, Hartmann ([4]) shows the relevance and the adventages of *Type I* indicators over the *Type II* for the adaptive mesh design for a supersonic flow past an airfoil.
The data for the adjoint problem is a quantity of interest depending on the application. In engineering applications, this is typically a functional of the analytical solution such as a mean, point value, boundary flux. In fluid dynamics, it may be the pression at the stagnation point, the pressure-drop between inflow and outflow or the drag or lift coefficients of a body immersed into the fluid.

# 2 Definition in continuous

**Primal problem model** Let $\Omega$ be a bounded open domain $R^d$ with boundary $\Gamma$. Given the *primal problem*

$$Lu = f \quad \text{in} \quad \Omega \qquad\qquad Bu = g \quad \text{on} \quad \Gamma \tag{1}$$

where $f \in L^2(\Omega)$ and $g \in L^2(\Gamma)$, $L$ denotes a linear differential operator on $\Omega$ and $B$ denotes a linear boundary operator on $\Gamma$.
To solve this problem a numerical discretization is given and an approximated solution, $u_h$, is sought in the place of $u$, by using a discrete numerical method. We consider the numerical solution as a linear combination of piecewise polynomial functions of degree $p$ on a partition $\mathcal{T}_h$ of the domain $\Omega$. For this reason we can write $u_h \in V_{h,p}$.

**The functional** $J(\cdot)$ In many problems of physical interest the quantity of interest for the current problem is an output or target functional of the solution rather the solution itself. This target functional is defined as $J(\cdot)$. Depending on the problem, it can be a different quantity, for example the drag or the lift coefficient or a point value of the solution.
This functional will be computed numerically and evaluated by the numerical solution, $J_h(u_h)$. The final purpose is to compute as good as possible this quantity, trying to estimate the order of error that the numerical approximations generate. Given a tolerance $\mathsf{TOL} > 0$, then the problem might be defined as finding $u_h \in V_{h,p}$ such that

$$|J(u) - J_h(u_h)| \leq \mathsf{TOL} \tag{2}$$

**Associated adjoint problem** Mathematical theory tells us that, by the (continuous) *compatibility condition*

$$(Lu, v)_\Omega + (Bu, C^*v)_\Gamma = (u, L^*v)_\Omega + (Cu, B^*v)_\Gamma \tag{3}$$

for each operator appearing in the primal problem, $L$, $B$ and $C$, there exists a corresponding adjoint one, $L^*$, $B^*$ and $C^*$. By these so-called *adjoint operators*, we build the adjoint problem associated to (1)

$$L^*z = j_\Omega \quad \text{in} \quad \Omega, \qquad\qquad B^*z = j_\Gamma \quad \text{on} \quad \Gamma. \tag{4}$$

Terms $j_\Omega$ and $j_\Gamma$ on the right-hand side depend on the target quantity that we want to investigate and that, according to the theory, it is defined as follows

$$J(\omega) = (\omega, j_\Omega)_\Omega + (C\omega, j_\Gamma)_\Gamma \tag{5}$$

where $j_\Omega \in L^2(\Omega)$ and $j_\Gamma \in L^2(\Gamma)$ and $C$ is a differential boundary operator on $\Gamma$.
The associated adjoint problem is hugely important. It provides how the information is transported towards the current quantity of interest. This property is extremely useful to derive where and how the source of the error of the target quantity is carried over the domain. The error indicator derived by this further information will be able to refine only the terms that really affect the error of the quantity of interest.

## 2.1 Linear advection-reaction

Let consider the linear advection-reaction problem

$$\nabla \cdot (\boldsymbol{b}u) + cu = f \quad \text{in} \quad \Omega \qquad\qquad u = g \quad \text{on} \quad \Gamma_- \tag{6}$$

where $f \in L^2(\Omega)$, $\boldsymbol{b} \in [C^1(\Omega)]^d$ and $\nabla \cdot \boldsymbol{b} = 0$, $c \in L^\infty(\Omega)$ and $g \in L^2(\Gamma_-)$, where

$$\Gamma_- = \{\boldsymbol{x} \in \Gamma, \quad \boldsymbol{b}(\boldsymbol{x}) \cdot \boldsymbol{n}(\boldsymbol{x}) < 0\}$$

denotes the inflow part of the boundary $\Gamma = \partial\Omega$.
So we find,

$$Lu = \nabla \cdot (\boldsymbol{b}u) + cu, \qquad Bu = \delta_{\Gamma_-} u, \qquad Cu = \delta_{\Gamma_+} u$$

where

$$\delta_{\Gamma_\pm} = \begin{cases} 1 & \text{if} \quad \boldsymbol{x} \in \Gamma_\pm \\ 0 & \text{otherwise} \end{cases}$$

Then, the (continuous) compatible condition becomes

$$(\nabla \cdot (\boldsymbol{b}u) + cu, z)_\Omega + (\delta_{\Gamma_-} u, -\boldsymbol{b} \cdot \boldsymbol{n} z)_\Gamma = (u, -\boldsymbol{b} \cdot \nabla z + cz)_\Omega + (\delta_{\Gamma_+} u, \boldsymbol{b} \cdot \boldsymbol{n} z)_\Gamma$$

with a linear target functional (5), the continuous adjoint problem is thus given by

$$-\boldsymbol{b} \cdot \nabla z + cz = j_\Omega \quad \text{in} \quad \Omega \qquad\qquad \boldsymbol{b} \cdot \boldsymbol{n}\, z = j_\Gamma \quad \text{on} \quad \Gamma_+ \tag{7}$$

so

$$L^* z = -\boldsymbol{b} \cdot \nabla z + cz, \qquad B^* z = \delta_{\Gamma_+} \boldsymbol{b} \cdot \boldsymbol{n} z, \qquad C^* z = -\delta_{\Gamma_-} \boldsymbol{b} \cdot \boldsymbol{n} z$$

As seen, depending on $j_\Omega$ and $j_\Gamma$ definitions a different functional is taken. Typical examples used for linear hyperbolic problems are

($i$) Outflow functional

$$J_{\text{out}}(u) = \int_\Gamma \delta_+ (\boldsymbol{b} \cdot \boldsymbol{n}) \psi u \, dl$$

with $\psi$ a enough smooth function.

1. Solution average functional

$$J_{\text{ave}}(u) = \int_\Omega u \, d\boldsymbol{x}$$

($ii$) Mollified pointwise functional

$$J_{\text{mol}}(u) = \int_\Omega \psi(r_0; |\boldsymbol{x} - \boldsymbol{x}_0|) u \, d\boldsymbol{x}$$

$$\psi(r_0; |\boldsymbol{x} - \boldsymbol{x}_0|) = \begin{cases} 0 & r \geq r_0 \\ \dfrac{e^{1/(r^2/r_0^2 - 1)}}{2\pi \int_0^{r_0} e^{1/(\xi^2/r_0^2 - 1)} \xi \, d\xi} & r < r_0 \end{cases}$$

# 3 Numerical discretization

Let $\Omega$ be subdivided into shape-regular mesh $\mathcal{K} = \{\kappa\}$ consisting of elements $\kappa$. Let $\mathcal{V}_{h,p}$ be the standard finite element space of piecewise polynomials of complete degree $p$ with $C^0$ continuity between elements

$$\mathcal{V}_{h,p} = \{v : v \in C^0(\Omega), v|_\kappa \in \mathcal{P}_p(\kappa), \forall \kappa \in \mathcal{K}\} \tag{8}$$

with $\mathcal{P}(\kappa)$ the space of polynomials of degree $\leq p$ defined on an element $\kappa$. Let then define a second space $\mathcal{V}^B_{h,q}$ which is the mesh dependent broken space of piecewise polynomials of complete degree $q$ in each $\kappa$ with no continuity between elements

$$\mathcal{V}^B_{h,q} = \{v : v|_\kappa \in \mathcal{P}_q(\kappa), \forall \kappa \in \mathcal{K}\} \tag{9}$$

Let discretize both problems and solve them numerically by using a *Petrov-Galerkin* (PG) method, where trial and test functions belong to $\mathcal{V}_{h,p}$ and $\mathcal{V}^B_{h,q}$, depending on the current problem.
According to (8) and (9), the boundary conditions are not included in the functional spaces and then, they are added and solved thorough the current problem. The approch with a strong formulation for the boundary conditions is hint in A.
Then following (3), the (discrete) compatibility condition holds as follows

$$\begin{gathered}(Lu_h, v_b)_\Omega + (Bu_h, C^* v_b)_\Gamma \\ = \\ (u_h, L^* v_b)_\Omega + (Cu_h, B^* v_b)_\Gamma + \sum_k (H(u_h, \boldsymbol{n}), v_B^+)_{\partial\kappa\setminus\Gamma}\end{gathered} \tag{10}$$

where $H(w_h, \boldsymbol{n})$ is the numerical flux over $\partial\kappa$, which is continuous because the $w_h \in \mathcal{V}_{h,p}$, $\boldsymbol{n}$ is the outward normal along the element boundary and $v_B^+$ the outward traces of $v_b$ over $\partial\kappa$.
So we can define a bilinear operator $\mathcal{B}(\cdot,\cdot)$ as

$$\mathcal{B}(u_h, v_b) = (Lu_h, v_b)_\Omega + (Bu_h, C^* v_b)_\Gamma \tag{11}$$

The (discrete) primal problem is then defined as

**PRIMAL PROBLEM** Find $u_h \in \mathcal{V}_{h,p}$ such that

$$\mathcal{B}(u_h, v_b) = F(v_b) \qquad \forall v \in \mathcal{V}^B_{h,q} \tag{12}$$

while the corresponding adjoint problem is given by

**ADJOINT PROBLEM** Find $z_B \in \mathcal{V}^B_{h,q}$ such that

$$\mathcal{B}(w_h, z_B) = J(w_h) \qquad \forall w_h \in \mathcal{V}_{h,p} \tag{13}$$

As we see, both problems use the same operator $\mathcal{B}(\cdot,\cdot)$ but in the primal one, the solution $u_h \in \mathcal{V}_{h,p}$ and the test function belongs to $\mathcal{V}^B_{h,q}$, while for the adjoint problem, the solution $z_B \in \mathcal{V}^B_{h,q}$ and the test function is taken from $\mathcal{V}_{h,p}$.

## 3.1 Broken space $\mathcal{V}_{h,q}^B$

A pletora of possible Broken spaces $\mathcal{V}_{h,q}^B$ are available. Herebelow let list the three Petrov-Galerkin spaces that will be taken into account for the next computations. Therefore, let remind that for a PG method, all of the broken spaces $\mathcal{V}_{h,q}^B$ can be always defined by a sum of two contributions

$$\mathcal{V}_{h,q}^B = \text{span}\{\Psi^0 + \Psi^1\}$$

where $\Psi^0$ is the "main" shape function of the space and $\Psi^1$ is a element stabilizer term.

**Streamline Upwind Petrov-Galerkin method** In case of a Stremline Upwind Petrov-Galerkin (SUPG) method, the broken space $\mathcal{V}_{h,q}^B$ is the same than $\mathcal{V}_{h,p}$ with still the addition of a stabilizer term

$$\mathcal{V}_{h,q}^B = \text{span}\{\varphi_i^q + \tau_\kappa \boldsymbol{b} \cdot \nabla \varphi_i^q\} \tag{14}$$

where $\tau_\kappa$ is usually the size of the element $\kappa$ and $\varphi_i^q$ the Lagrange interpolant polynomial of the degree of freedom, $i$, and order $q$; while, fanally, $\boldsymbol{b}$ is the local advection of the current problem. So for this functional space $\Psi_j^0 = \varphi_j^q$ and $\Psi_j^1 = \tau_\kappa \boldsymbol{b} \cdot \nabla \varphi_j^q$.

**Residual-Distribution Method** If the stabilised Residual Distribution (RD) space is chosen, the broken space, $\mathcal{V}_{h,q}^B$, is defined as

$$\begin{aligned} \mathcal{V}_{h,q}^B &= \text{span}\{\chi^\kappa \beta_i^\kappa\} && \text{for} \quad q = 1 \\ \mathcal{V}_{h,q}^B &= \text{span}\{\chi^\kappa \beta_i^\kappa + \tau_\kappa \boldsymbol{b} \cdot \nabla \varphi_i^q\} && \text{for} \quad q > 1 \end{aligned} \tag{15}$$

where $\beta_i^\kappa \in C^0$, $\chi^\kappa$ is 1 in $\kappa$ and 0 everywhere else, while $\tau_\kappa$ is usually the size of the element $\kappa$ and $\varphi_i^q$ the Lagrange interpolant polynomial of the degree of freedom, $i$, and order $q$. So $\Psi_j^0 = \chi^\kappa \beta_j^\kappa$ and $\Psi_j^1 = 0$ or $\tau_\kappa \boldsymbol{b} \cdot \nabla \varphi_j^q$.

**"Bubble" method** The "bubble" method comes out from the equivalence of the RD and SUPG method. Indeed, it takes the following broken space $\mathcal{V}_{h,q}^B$

$$\mathcal{V}_{h,q}^B = \text{span}\{\varphi_i^q + S^\kappa \alpha_i^\kappa\} \tag{16}$$

where $\varphi_i^q$ the Lagrange interpolant polynomial of the degree of freedom, $i$, and order $q$, while $S^\kappa$ is a bubble function null along $\partial\kappa$. In this case, it is either a linear bubble, unary in the baricentric point $\boldsymbol{x}_g$, or a cubic one, coming out from the product of the three vertex linear functions. Finally $\alpha_i^\kappa$ is given by $\alpha_i^\kappa = \beta_i - \phi_i$, where $\beta_i$ is the corresponding RD basis function. Then here $\Psi_j^0 = \varphi_j^q$ and $\Psi_j^1 = S^\kappa \alpha_i^\kappa$.

## 3.2 Numerical analysis

**Consistency and adjoint consistency** All Petrov-Galerkin methods hold the *Galerkin orthogonality*

$$\mathcal{B}(u - u_h, v_b) = 0 \qquad \forall v \in \mathcal{V}_{h,p}^b \tag{17}$$

which means that the discretization error $e = u - u_h$ is orthogonal (with respect to the bilinear form $\mathcal{B}$) to the discrete test space $\mathcal{V}^b_{h,p}$. Hence, because $v \in \mathcal{V}^b_{h,p} \subset \mathcal{V}$, we find

$$\mathcal{B}(u, v) = F(v) \qquad \forall v \in \mathcal{V} \tag{18}$$

This proves that a PG method is a *consistent* discretization of the primal problem (1). Furthermore, a numerical discretization is called also *adjoint consistent* [5], if the exact solution $z \in \mathcal{V}$ to the adjoint problem (4) satisfies

$$\mathcal{B}(w, z) = J(w) \qquad \forall w \in \mathcal{V} \tag{19}$$

In other words, if the discrete adjoint problem is a consistent discretization of the continuous adjoint problem. Motivated by the identity (10) and replcing $z_B$ by the exact solution $z$ and because $w_h \in \mathcal{V}_{h,p} \subset \mathcal{V}$, we can state that the bilinear form $\mathcal{B}$ is also adjoint consistent.

**Convergence (order of convergence)** Let $u \in H^{p+1}(\Omega)$ and $u_h \in \mathcal{V}_{h,p}$ be the solutions to (18) and (1), respectively. Then,

$$||u - u_h||_{L^2(\Omega)} \leq Ch^{p+1}|u|_{H^{p+1}(\Omega)} \tag{20}$$

Let $p \geq 0$ and $\mathcal{V}^b_{h,p}$ be the broken finite element space defined in (9). Then, by $P^b_{h,p}$ we denote the $L^2$-projection onto $\mathcal{V}^b_{h,p}$, i.e. given a $u \in L^2(\Omega)$ we define $P^b_{h,p}u \in \mathcal{V}^b_{h,p}$ by

$$\int_\Omega \left(u - P^b_{h,p}u\right) v_h \, d\boldsymbol{x} = 0 \quad \forall v_h \in \mathcal{V}^b_{h,p}$$

we use the short notation $P_h u$ instead of $P^b_{h,p}u$ when is clear which projection is meant. Now, let $p \geq 0$ and $P_h v$ be the $L^2$-projection. Suppose $v \in H^{p+1}(\Omega)$, then

$$||v - P_h v||_{H^{p+1}(\Omega)} \leq Ch||v||_{L^2(\Omega)} \tag{21}$$

To numercally verify the convergence rate for smooth primal and adjoint data, numerical solutions of the following 2-D advection problem [6] were obtained

$$\begin{aligned} \boldsymbol{b} \cdot \nabla u &= 0 \quad \text{in } \Omega \\ u &= g \quad \text{on } \Gamma \end{aligned} \tag{22}$$

with circular advection field $\boldsymbol{b} = (-y, x)$ and

$$g(x) = \begin{cases} \tilde{\psi}(9/20; |x - 1/2|)(1 - \tilde{\psi}(9/20; |x - 1/20|)) & y = 0, x \leq 1/2 \\ \tilde{\psi}(9/20; |x - 1/2|)(1 - \tilde{\psi}(9/20; |x - 19/20|)) & y = 0, x > 1/2 \\ 0 & \text{otherwise} \end{cases}$$

where $\tilde{\psi}(:;:)$ is a $C^\infty$ function

$$\tilde{\psi}(r_0; r) = \begin{cases} 0 & r \geq r_0 \\ e^{1/(r^2/(r^2 - r_0^2))} & r < r_0 \end{cases}$$

The target quantity is the weighted outflow flux functional

$$J(u) = \int_0^1 \delta_+(\boldsymbol{b} \cdot \boldsymbol{n}) \psi_{\text{outflow}} u \, d\boldsymbol{x}$$

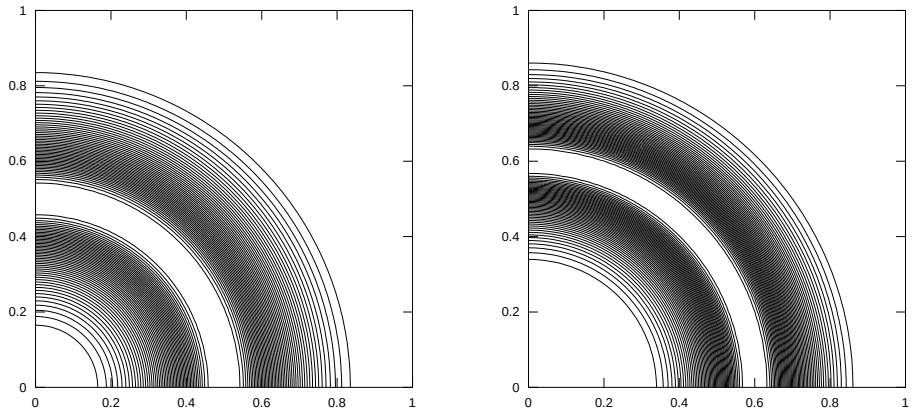


**(a)** **(b)**

**Figure 1:** Barth's problem : (a) primal; (b) adjoint

with weighting function

$$\psi_{\text{outflow}}(y) = \begin{cases} \tilde{\psi}(7/20; |x-3/5|)(1-\tilde{\psi}(7/20; |x-1/4|)) & x=0, y \leq 3/5 \\ \tilde{\psi}(7/20; |x-3/5|)(1-\tilde{\psi}(7/20; |x-19/20|)) & x=0, y > 3/5 \\ 0 & \text{otherwise} \end{cases}$$

Figures 1a and 1b draw primal and adjoint current solutions, respectively, while table 1. tabulates values of the global solution error using a sequence of four nested meshes. Here, the $p+1$ convergence rate for the $u$ solution error is satisfied and so the rate for the adjoint solution. In this case, the latter rate is even better than the expected one from (25). The SUPG scheme keep the same convergence rate for both solutions, while the other schemes RD-LDA and BUBBLE show a order 2 for $p=1$ and 1 for $p>1$.
Let now examinate the convergence rates for functionals. We consider the general linear problem (1) and its numerical discretization (12), where the bilinear form $\mathcal{B}(\cdot,\cdot)$ is continuous on $\mathcal{V}$ with respect to a specific $|||\cdot|||$-norm, i.e.

$$\mathcal{B}(w,v) \leq C_B |||\, w \,||| \, |||\, v \,||| \quad \forall w, v \in \mathcal{V} \tag{23}$$

Because the discretization is consistent and thus, the Galerkin orthogonality is satisfied, we assume that following *a priori* error estimate in the $|||\cdot|||$-norm holds: there are constants $C>0$ and $r=r(p)>0$ such that

$$|||\, u-u_h \,||| \leq Ch^r |u|_{H^{p+1}(\Omega)} \quad \forall u \in H^{p+1}(\Omega) \tag{24}$$

Finally, we assume that the projection operator $P^b_{h,p}$ satisfies following approximation estimate in the $|||\cdot|||$-norm: there are constants $C>0$ such that

$$|||\, v - P^b_{h,p} v \,||| \leq Ch||v||_{L^2(\Omega)} \quad \forall v \in L^2(\Omega) \tag{25}$$

| Method | h | $\|\|u-u_h\|\|_{L^2}$ | | $\|\|z-z_h\|\|_{L^2}$ | | $\|J(u)-J(u_h)\|$ | |
|---|---|---|---|---|---|---|---|
| SUPG | .0312 | 3.741e-03 | | 5.239e-03 | - | 7.402e-05 | |
| SUPG | .0156 | 8.815e-04 | (2.08) | 1.839e-03 | (1.51) | 1.105e-05 | (2.74) |
| SUPG | .0078 | 1.552e-04 | (2.50) | 3.590e-04 | (2.36) | 1.438e-06 | (2.94) |
| SUPG | .0039 | 2.578e-05 | (2.59) | 6.275e-05 | (2.52) | 1.803e-07 | (3.00) |
| RD-LDA | .0312 | 3.675e-03 | | 7.739e-03 | - | 2.188e-04 | |
| RD-LDA | .0156 | 1.092e-03 | (1.75) | 2.765e-03 | (1.48) | 5.968e-05 | (1.87) |
| RD-LDA | .0078 | 2.871e-04 | (1.93) | 7.869e-04 | (1.81) | 1.599e-05 | (1.90) |
| RD-LDA | .0039 | 7.335e-05 | (1.97) | 2.260e-04 | (1.80) | 4.128e-06 | (1.95) |
| BUBBLE | .0312 | 2.635e-03 | | 4.661e-03 | - | 1.003e-04 | |
| BUBBLE | .0156 | 6.100e-04 | (2.11) | 1.492e-03 | (1.64) | 2.736e-05 | (1.87) |
| BUBBLE | .0078 | 1.472e-04 | (2.05) | 3.692e-04 | (2.01) | 7.201e-06 | (1.93) |
| BUBBLE | .0039 | 3.582e-05 | (2.04) | 1.011e-04 | (1.87) | 1.841e-06 | (1.97) |

**Table 1:** Convergence rates $p = 1$ order of SUPG, RD and BUBBLE methods : circular advection problem [6].

Let then assume that the target quantity as described in (5) with $j_\Omega$ and $æ_\Gamma$ smooth functions on $\Omega$ and $\Gamma$, respectively. Then we have following estimate

$$\begin{aligned} |J(u)-J(u_h)| = |\mathcal{B}(u-u_h,z)| = |\mathcal{B}(u-u_h, z-P^b_{h,p}z)| \\ \leq Ch^{r+1}|u|_{H^{p+1}(\Omega)}||v||_{L^2(\Omega)} \end{aligned} \tag{26}$$

Once again, to numerically verify the convergence rate of functionals for a Petrov-Galerkin scheme let consider the circular advection problem [6] whose results are tabulated on tables 1 and 2.
The $p+1$ order for the functional error is satisfied by RD and BUBBLE schemes, while for SUPG a superconvergence rate $2p+1$ is obtained. This behaviour seems to be strictly connected to the higher order of the corresponding adjoint solution of this scheme.

# 4 Error Representation Formula

Let consider the primal numerical problem (12) and that holds the *Galerkin orthogonality condition* (17). Let then notice that by the *compatibility condition* (3), using infinite-dimentional trial and test space, the adjoint problem can be redefined as

$$\mathcal{B}(w,z) = J(w) \qquad \forall w \in \mathcal{V}$$

So, an exact error representation formula for a given functional $J(\cdot)$ results from the following steps, where $P_h$ denotes any suitable projection operator (i.e. interpolation,

| Method | h | $\|\|u-u_h\|\|_{L^2}$ | | $\|\|z-z_h\|\|_{L^2}$ | | $\|J(u)-J(u_h)\|$ | |
|---|---|---|---|---|---|---|---|
| SUPG | .0312 | 2.624e-04 | | 7.040e-04 | - | 5.785e-07 | |
| SUPG | .0156 | 3.243e-05 | (3.01) | 9.713e-05 | (2.86) | 2.236e-08 | (4.69) |
| SUPG | .0078 | 2.887e-06 | (3.49) | 1.057e-05 | (3.20) | 7.620e-10 | (4.88) |
| SUPG | .0039 | 3.138e-07 | (3.20) | 1.141e-06 | (3.21) | 2.412e-11 | (4.98) |
| RD-LDA | .0312 | 3.773e-04 | | 8.681e-03 | - | 1.609e-06 | |
| RD-LDA | .0156 | 8.095e-05 | (2.22) | 4.951e-03 | (0.81) | 2.067e-07 | (2.96) |
| RD-LDA | .0078 | 1.544e-05 | (2.39) | 2.728e-03 | (0.86) | 2.869e-08 | (2.85) |
| RD-LDA | .0039 | 2.533e-06 | (2.61) | 1.481e-03 | (0.88) | 3.613e-09 | (2.99) |
| BUBBLE | .0312 | 1.806e-04 | | 7.148e-03 | - | 3.907e-06 | |
| BUBBLE | .0156 | 3.800e-05 | (2.25) | 4.569e-03 | (0.65) | 6.089e-07 | (2.68) |
| BUBBLE | .0078 | 8.347e-06 | (2.19) | 2.720e-03 | (0.75) | 8.231e-08 | (2.89) |
| BUBBLE | .0039 | 1.645e-06 | (2.34) | 1.525e-03 | (0.83) | 1.063e-08 | (2.95) |

**Table 2:** Convergence rates $p = 2$ order of SUPG, RD and BUBBLE methods : circular advection problem [6].

$L_2$ projection) into $\mathcal{V}^b_{h,p}$,

$$\begin{aligned} J(u) - J(u_h) &= J(u-u_h) && \text{(linearity } J\text{)} \\ &= \mathcal{B}^*(z, u-u_h) && \text{(adjoint problem)} \\ &= \mathcal{B}(u-u_h, z) && \text{(compatibility condition)} \\ &= \mathcal{B}(u-u_h, z-P_h z) && \text{(orthogonality)} \\ &= \mathcal{B}(u, z-P_h z) - \mathcal{B}(u_h, z-P_h z) && \text{(linearity } \mathcal{B}\text{)} \\ &= F(z-P_h z) - \mathcal{B}(u_h, z-P_h z) && \text{(primal problem)} \end{aligned} \tag{27}$$

so in summary

$$J(u) - J(u_h) = F(z-P_h z) - \mathcal{B}(u_h, z-P_h z) \tag{28}$$

where no dependence on the exact solution $u$ appears.
Comptutationally, this error representation formula is not suitable for obtaing computable *a posteriori* error estimation unless the function $z - P_h z$ is unknown, since $z \in \mathcal{V}^B$ is a solution of the infinite-dimensional adjoint problem. So $z$ has to be computed by the discrete adjoint problem (13). Since the (10), we can solve the adjoint problem by using the same bilinear operator, $\mathcal{B}(w_h, z)$, used for the primal problem. Due to the Galerkin orthogonality, the adjoint numerical problem must be approximated in a larger space of functions than that utilized in the primal numerical problem. Here, this is achieved by solving the adjoint problem using a polynomial space that is one polynomial degree higher than the primal numerical problem, i.e. if $v_b \in \mathcal{V}^B_{h,q}$ then $z \approx z_{B'} \in \mathcal{V}^B_{h,q+1}$.
The error representation formula written in the global abstract form of the (28) does not indicate which elements in the mesh should be refined to reduce the measured error

in a functional. So, now the goal is to estimate the *local* contribution of each element in the mesh to the functional error. This local cell contribution will then be used as an error indicator for choosing which elements to refine or coarsen in the adaptive mesh procedure. By applying the *triangle inequality*, indeed, we have

$$\begin{aligned}
\big|J(u) - J(u_h)\big| &= \big|F(z - P_h z) - \mathcal{B}(u_h, z - P_h z)\big| && \text{(error representation)} \\
&= \Big|\sum_{\kappa\in\mathcal{K}} F_\kappa(z - P_h z) - \mathcal{B}_\kappa(u_h, z - P_h z)\Big| && \text{(element assembly)} \\
&\leq \sum_{\kappa\in\mathcal{K}} \big|F_\kappa(z - P_h z) - \mathcal{B}_\kappa(u_h, z - P_h z)\big| && \text{(triangle inequality)}
\end{aligned} \tag{29}$$

where

$$\begin{aligned}
F_\kappa(z - P_h z) - \mathcal{B}_\kappa(u_h, z - P_h z) &= (f - Lu, z - P_h z)_\kappa + (g - Bu, C^*(z - P_h z))_{\partial\kappa\cap\Gamma} \\
&= \mathcal{R}_\kappa(u_h, z - P_h z)
\end{aligned}$$

and

$$\mathcal{R}_\kappa(u, v) = (R(u), v)_\kappa + (r(u), C^* v)_{\partial\kappa\cap\Gamma}$$

with $R(u) = f - Lu$ and $r(u) = g - Bu$.

**Adaptive Meshing** This direct estimate let us define for each partition element $\kappa$ the *adaptation element indicator* $\eta_\kappa$

$$|\eta_\kappa| \equiv \big|\mathcal{R}_\kappa(u_h, z - P_h z)\big| \tag{30}$$

such that the simplest adaptation stopping criteria will be

$$|J(u) - J(u_h)| = \Big|\sum_\kappa \eta_\kappa\Big|$$

Hence, a simple mesh adaptation strategy can be outlined as follows:

1. Construct an initial mesh $\mathcal{K}$
2. Compute the numerical approximation of the primal problem on the current mesh $\mathcal{K}$
3. Compute the numerical approximation of the adjoint problem on the current mesh $\mathcal{K}$
4. Compute error indicators, $\eta_\kappa$, for all elements $\kappa \in \mathcal{K}$
5. If $|\sum_{\kappa\in\mathcal{K}} \eta_\kappa| < \mathsf{TOL}$ where $\mathsf{TOL}$ is a given tolerance, then STOP
6. Otherwise, refine and coarsen a specified fraction of the total numeber of elements according to the size of $|\eta_\kappa|$, generate a new mesh $\mathcal{K}$ and GOTO 2

| Method | h | $\lvert J(u) - J(u_h)\rvert$ | $\lvert \sum_\kappa \eta_\kappa \rvert$ | $(\theta_{\text{eff}})$ | $\sum_\kappa \lvert \eta_\kappa \rvert$ | $(\theta_{\text{eff}})$ |
|---|---|---|---|---|---|---|
| SUPG | .0312 | 7.402e-05 | 7.402e-05 | (1.00) | 1.604e-04 | (2.17) |
| SUPG | .0156 | 1.105e-05 | 1.106e-05 | (1.00) | 2.231e-05 | (2.02) |
| SUPG | .0078 | 1.438e-06 | 1.439e-06 | (1.00) | 2.829e-06 | (1.97) |
| SUPG | .0039 | 1.803e-07 | 1.804e-07 | (1.00) | 3.538e-07 | (1.96) |
| RD-LDA | .0312 | 2.188e-04 | 2.202e-04 | (1.01) | 5.445e-04 | (2.49) |
| RD-LDA | .0156 | 5.968e-05 | 5.974e-05 | (1.00) | 1.321e-04 | (2.21) |
| RD-LDA | .0078 | 1.599e-05 | 1.599e-05 | (1.00) | 3.306e-05 | (2.07) |
| RD-LDA | .0039 | 4.128e-06 | 4.128e-06 | (1.00) | 8.234e-06 | (2.00) |
| BUBBLE | .0312 | 1.003e-04 | 1.032e-04 | (1.03) | 2.490e-04 | (2.48) |
| BUBBLE | .0156 | 2.736e-05 | 2.786e-05 | (1.02) | 6.089e-05 | (2.23) |
| BUBBLE | .0078 | 7.201e-06 | 7.266e-06 | (1.01) | 1.514e-05 | (2.10) |
| BUBBLE | .0039 | 1.841e-06 | 1.849e-06 | (1.00) | 3.740e-06 | (2.03) |

**Table 3:** Efficiency rates $p_{\text{p}} = 1$ and $p_{\text{a}} = 2$ order of the SUPG, RD and BUBBLE methods error estimates : circular advection problem [6].

# 5 Numerical Results

In this section, selected numerical examples are given for scalar advection (and/or reaction) problems. SUPG, RD and bubble schemes are the numerical schemes used for all cases. The following tables tabulate values of the functional error and the estimated error as given in (29) using numercally approximated adjoint problems.
In addition, an effictivity index is included to characterize the sharpness of the current estimates

$$\theta_{\text{eff}} = \frac{|\text{estimated error}|}{|J(u) - J(u_h)|} \tag{31}$$

When the exact adjoint solution is used

$$|J(u) - J(u_h)| = \Big| \sum_{\kappa \in \mathcal{K}} \eta_\kappa \Big| \equiv |\mathcal{E}_\Omega|$$

so the corresponding column in the following tables measures the effect of numerically approximating the adjoint problem. After application of the triangle inequality, the estimate

$$|J(u) - J(u_h)| \leq \sum_{\kappa \in \mathcal{K}} |\eta_\kappa| \equiv \mathcal{E}_{|\Omega|}$$

is obtained. Mesh adaptation strategies are usually based on $|\eta_\kappa|$ and so they depend on this error estimation. As internal cancellations are precluded, the estimate can usually lose in accuracy. Hence, column eight and nine of the following tables show the current estimate and its efficiency index.

| Method | h | $\lvert J(u) - J(u_h)\rvert$ | $\lvert\sum_\kappa \eta_\kappa\rvert$ | $(\theta_{\text{eff}})$ | $\sum_\kappa \lvert\eta_\kappa\rvert$ | $(\theta_{\text{eff}})$ |
|---|---|---|---|---|---|---|
| SUPG | .0312 | 5.785e-07 | 5.727e-07 | (.990) | 9.610e-07 | (1.66) |
| SUPG | .0156 | 2.236e-08 | 2.237e-08 | (1.00) | 3.826e-08 | (1.71) |
| SUPG | .0078 | 7.620e-10 | 7.628e-10 | (1.00) | 1.340e-09 | (1.76) |
| SUPG | .0039 | 2.412e-11 | 2.441e-11 | (1.01) | 4.359e-11 | (1.81) |
| RD-LDA | .0312 | 1.609e-06 | 1.601e-06 | (.995) | 1.890e-05 | (11.7) |
| RD-LDA | .0156 | 2.067e-07 | 2.154e-07 | (1.04) | 3.037e-06 | (14.7) |
| RD-LDA | .0078 | 2.869e-08 | 2.937e-08 | (1.02) | 4.393e-07 | (15.3) |
| RD-LDA | .0039 | 3.613e-09 | 3.659e-09 | (1.01) | 5.961e-08 | (16.5) |
| BUBBLE | .0312 | 3.907e-06 | 3.997e-06 | (1.02) | 8.059e-06 | (2.06) |
| BUBBLE | .0156 | 6.089e-07 | 6.140e-07 | (1.01) | 1.300e-06 | (2.14) |
| BUBBLE | .0078 | 8.231e-08 | 8.267e-08 | (1.00) | 2.370e-07 | (2.88) |
| BUBBLE | .0039 | 1.063e-08 | 1.066e-08 | (1.00) | 3.907e-08 | (3.67) |

**Table 4:** Efficiency rates primal $p_{\text{p}} = 2$ and $p_{\text{a}} = 3$ order of the SUPG, RD and BUBBLE methods error estimates : circular advection problem [6].

**Circular advection** The circular advection problem given in [6] is again considered. As we have already seen, both primal and adjoint solutions are enough smooth functions and then, their corresponding convergence rate (tables 1 and 2) follows the theoretical rate. The smoothness condition leads also the first error estimation ($|\mathcal{E}_\Omega|$) to converge towards the exact functional error ($\theta_{\text{eff}} \approx 1$ for all schemes) and also to hold the second estimate ($\mathcal{E}_{|\Omega|}$), where only the RD with $p_{\text{p}} = 2$ and $p_{\text{a}} = 3$ gives $\theta_{\text{eff}}$ bigger than 10.

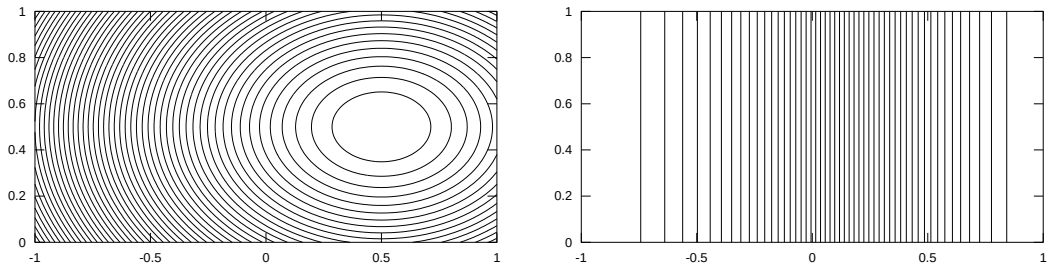


**Figure 2:** Reaction problem : (a) primal; (b) adjoint

| Method | h | $\lvert J(u) - J(u_h)\rvert$ | $\lvert\sum_\kappa \eta_\kappa\rvert$ | $(\theta_{\text{eff}})$ | $\sum_\kappa \lvert\eta_\kappa\rvert$ | $(\theta_{\text{eff}})$ |
|---|---|---|---|---|---|---|
| SUPG | .0625 | 4.497e-07 | 1.247e-07 | (.277) | 8.753e-06 | (19.5) |
| SUPG | .0312 | 4.903e-08 | 8.227e-08 | (1.68) | 1.793e-06 | (36.6) |
| SUPG | .0156 | 5.465e-09 | 1.517e-08 | (2.78) | 4.015e-07 | (73.5) |
| SUPG | .0078 | 6.322e-10 | 2.211e-09 | (3.50) | 9.448e-08 | (149) |
| RD-LDA | .0625 | 2.378e-05 | 2.502e-05 | (1.05) | 2.599e-05 | (1.04) |
| RD-LDA | .0312 | 5.955e-06 | 6.341e-06 | (1.07) | 6.601e-06 | (1.11) |
| RD-LDA | .0156 | 1.491e-06 | 1.598e-06 | (1.07) | 1.662e-06 | (1.12) |
| RD-LDA | .0078 | 3.731e-07 | 4.011e-07 | (1.08) | 4.170e-07 | (1.12) |
| BUBBLE | .0625 | 5.918e-06 | 9.453e-06 | (1.60) | 1.000e-05 | (1.69) |
| BUBBLE | .0312 | 1.456e-06 | 2.197e-06 | (1.51) | 2.330e-06 | (1.60) |
| BUBBLE | .0156 | 3.610e-07 | 5.292e-07 | (1.47) | 5.613e-07 | (1.56) |
| BUBBLE | .0078 | 8.988e-08 | 1.298e-07 | (1.45) | 1.376e-07 | (1.53) |

**Table 5:** Efficiency rates $p_{\text{p}} = 1$ and $p_{\text{a}} = 2$ order of the SUPG, RD and BUBBLE methods error estimates for the advection reaction problem.

**Advection-reaction** The advection-reaction case is defined by the following linear equation

$$\begin{aligned} \boldsymbol{b} \cdot \nabla u + cu &= f \quad \text{in } \Omega \\ u &= g \quad \text{on } \Gamma_- \end{aligned} \tag{32}$$

with $\boldsymbol{b} = (1, 0)$, $c = 1 - \text{sign}(x)x$. The source term $f$ is given such that the analytical solution $u^*$ of (32) is as follows

$$u^* = \alpha e^{-[a(x-x_0)^2 + b(y-y_0)^2]}$$

Finally, boundary conditions are consistent by the analytical solution. Once again the target quantity is an outflow functional such that the corresponding adjoint problem becomes

$$\begin{aligned} \boldsymbol{b} \cdot \nabla z + cz &= 0 \quad \text{in } \Omega \\ z &= 1 \quad \text{on } \Gamma_+ \end{aligned}$$

Figures 2a and 2b show primal and adjoint solutions, respectively, while error estimation data are tabulated on tables 5. and 6.. Here, RD-LDA scheme seem to be the best scheme, with all estimates which keep close to exact functional error. What sounds weird is the $p = 1$ SUPG estimate which seems out of control. This becomes even more weird by looking to the $p = 2$ estimate where both thetas converge to one.

## Adaptive mesh comparison :

With the follwing examples, we compare the efficency of the adjoint based error estimation, in adaptive meshing, with respect to the *ad hoc* estimation procedure.

| Method | h | $\lvert J(u) - J(u_h)\rvert$ | $\lvert\sum_\kappa \eta_\kappa\rvert$ | $(\theta_{\text{eff}})$ | $\sum_\kappa \lvert\eta_\kappa\rvert$ | $(\theta_{\text{eff}})$ |
|---|---|---|---|---|---|---|
| SUPG | .0625 | 7.432e-08 | 6.588e-08 | (.886) | 9.519e-08 | (1.28) |
| SUPG | .0312 | 1.012e-08 | 9.450e-09 | (.934) | 1.233e-08 | (1.22) |
| SUPG | .0156 | 1.318e-09 | 1.270e-09 | (.964) | 1.567e-09 | (1.19) |
| SUPG | .0078 | 1.679e-10 | 1.648e-10 | (.981) | 1.973e-10 | (1.18) |
| RD-LDA | .0625 | 2.087e-08 | 1.705e-08 | (.817) | 3.007e-08 | (1.44) |
| RD-LDA | .0312 | 2.604e-09 | 2.419e-09 | (.929) | 3.738e-09 | (1.44) |
| RD-LDA | .0156 | 3.214e-10 | 3.189e-10 | (.992) | 4.709e-10 | (1.47) |
| RD-LDA | .0078 | 3.968e-11 | 4.071e-11 | (1.03) | 5.895e-11 | (1.49) |
| BUBBLE | .0625 | 1.331e-08 | 3.364e-08 | (2.53) | 3.688e-08 | (2.77) |
| BUBBLE | .0312 | 1.544e-09 | 4.676e-09 | (3.03) | 5.106e-09 | (3.31) |
| BUBBLE | .0156 | 1.828e-10 | 6.179e-10 | (3.38) | 6.729e-10 | (3.68) |
| BUBBLE | .0078 | 2.196e-11 | 7.928e-11 | (3.61) | 8.713e-11 | (3.97) |

**Table 6:** Efficiency rates $p_{\text{p}} = 2$ and $p_{\text{a}} = 3$ order of the SUPG, RD and BUBBLE methods error estimates for the advection reaction problem.

**Hartmann's problem** Let consider the linear hyperbolic problem ([4]):

$$\begin{aligned} \boldsymbol{b}\cdot\nabla u &= f \quad \text{in } \Omega \\ u &= g \quad \text{on } \Gamma_- \end{aligned} \tag{33}$$

with the advection $\boldsymbol{b} = \frac{\tilde{\boldsymbol{b}}}{|\tilde{\boldsymbol{b}}|}$, where

$$\tilde{\boldsymbol{b}} = \begin{cases} (y, -x), & \text{for } x < 1, \\ (2-y, x) & \text{otherwise} \end{cases}$$

While, the boundary function, $g$, is defined as follows

$$g(x,y) = \begin{cases} 1, & \text{for } -7/8 \le x \le -1/4, \quad y = 0 \\ 0, & \text{otherwise} \end{cases}$$

The analytical solution is shown in figure 3a, where the two discontinuites of the two inlet jumps are carried along the charactistic directions of the advection field. Let then suppose to be interested in the solution along the outlet boundary segment $1/4 \le y \le 1$, with a wieght-function $\psi$

$$\psi(x,y) = \begin{cases} \exp\left(\left(\frac{3}{8}\right)^{-2} - \left[\left(y - \frac{5}{8}\right)^2 - \frac{3}{8}\right]^{-2}\right), & \text{for } x = 1, \quad 1/4 \le y \le 1 \\ 0, & \text{otherwise} \end{cases}$$

We solve numerically both problems by the RD-LDA scheme $p = 2$ and $p = 3$ order, respectively for primal and adjoint problem. Figure 4 shows the numerical solutions

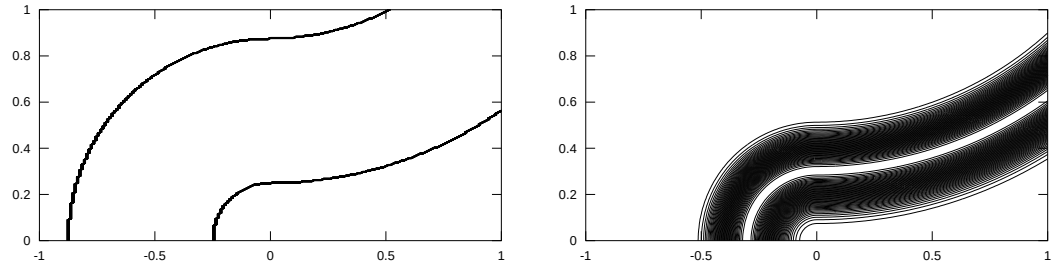


**(a)** **(b)**

**Figure 3:** Analytical solutions linear hyperbolic problem [4]: (a) primal; (b) adjoint

and the corresponding final adaptive meshes, generated by the *ad hoc* residual error indicators, $\eta_\kappa^{\text{ad hoc}}$, and the current adjoint weighted-ones, $\eta_\kappa^{\text{adj}}$, respectively. In figure 4c we see how the final mesh is refined along both discontinuites, giving a very good resolution for the both corresponding jumps, see figure 4a. Instead, the mesh coming out from the based adjoint error estimation refines only in the neighborhood of the lower jump, see figure 4d, the one which goes out through the target outlet. The other jump is then rougthly solved but, as the adjoint solution over that zone is null, the error of the solution along the second jump do not affect the current target quantity. This is the reason why it is not refined during the adaptation.
Comparing the two procedures, the adjoint-based estimation proves to be more efficient, since it reaches a similar accuracy of the target quantity: $|J(e)| = 1.1860 \times 10^{-6}$ vs. $|J(e)| = 1.7871 \times 10^{-6}$, generating a final mesh with rougthly half of the elements: $11753$ instead of $26307$. Moreover, figure 5 shows how the target quantity error of the adjoint refinement keeps always slightly inferior than the *ad hoc* one. However, we must to remind that this algorithm needs to solve two problems, primal and adjoint, while the simple based-residual estimation solve the only primal one. Since, in this case, both problems are linear and the adjoint is solved with an higher order, the added computational cost can be remarkable. Anyway, this cost will become negligiable for non-linear primal problem as the adjoint will be still linear.

**Circular-reaction problem** Let now consider the following advection-reaction problem:

$$\begin{aligned} \boldsymbol{b} \cdot \nabla u + cu &= f \quad \text{in } \Omega \\ u &= g \quad \text{on } \Gamma_- \end{aligned} \tag{34}$$

with $\boldsymbol{b} = (y, -x)$, $c = r \equiv \sqrt{x^2 + y^2}$ and the source term, $f$, and the boundary conditions, $g$, such that the solution is

$$u^* = \alpha e^{-[a(r-x_0)^2 + br_0^2(\theta-\theta_0)^2]}$$

with $\alpha = 1$, $a = 0.125$, $b = 0.250$, $r_0 = 0.5$ and $\theta = \pi/4$. Let then suppose to be interested in the solution along the bottom outlet boundary, $\Gamma_{\text{bo}} = [0, 1] \times \{0\}$, by imposing a wieght-function, $\tilde{\psi}(0.25; |x - 0.5|)$. The exact solutions are shown in figure 6.

We numerically solve both problems by the SUPG scheme $p = 1$ and $p = 2$ order,

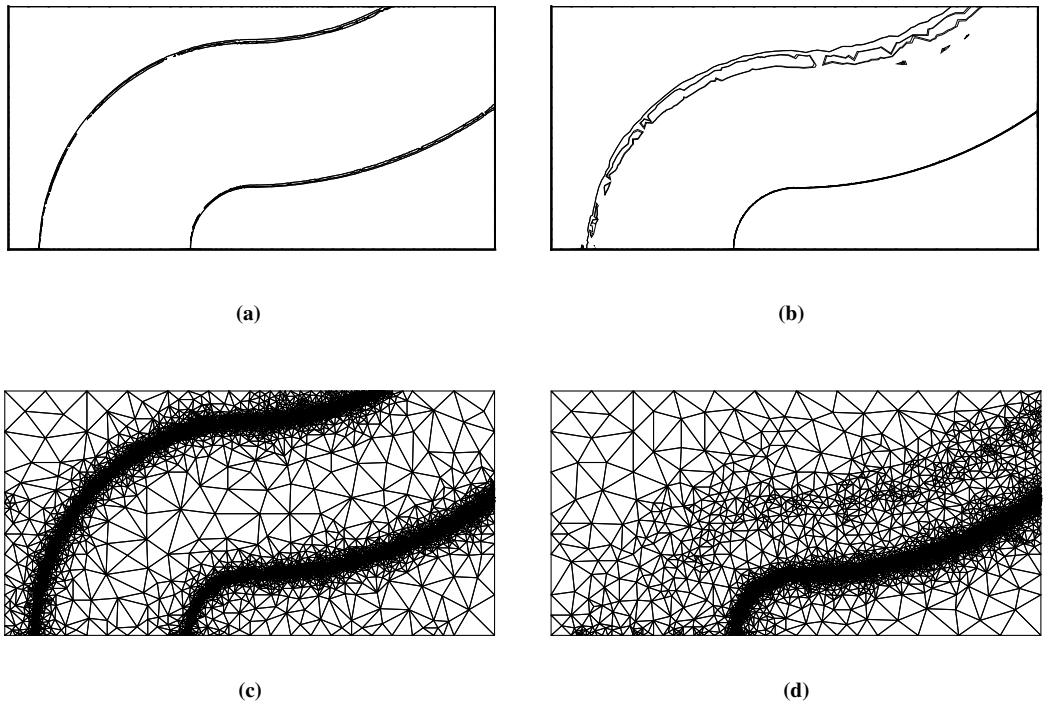

**Figure 4:** Adaptive refinement for the hyperbolic linear problem (33): (a) Numerical solution solved on the mesh (c), generated by a based-residual error estimation; (b) Numerical solution solved on the mesh (d), generated by the adjoint error estimation;

respectively for primal and adjoint problem. Figure 7 shows the initial and final adaptive meshes, generated by the *ad hoc* residual error indicators, $\eta_\kappa^{\text{ad hoc}}$, and the current adjoint weighted-ones, $\eta_\kappa^{\text{adj}}$, respectively. The *ad hoc* final mesh is pratically refined everywhere, figure 7b; while, the adjoint final mesh refines only in the neighborhood of the backward adjoint stream, see figure 7c.
Comparing the two efficencies, the *ad hoc* estimation reaches a target quantity error $|J(e)| = 1.7023 \times 10^{-7}$ with $2822$ elements; instead the adjoint-based estimation achieves $|J(e)| = 1.7897 \times 10^{-7}$ with only $1668$ elements.

# 6 Conclusions

Among different types of error representation formula, we interested in Type I error indicator. Unlike Type II error bounds where the only local residual is taken into account, Type I involves also the solution of the associated adjoint problem. By it, we are able to obtain further information concerning the trasport of the error of computing the quantity of interest.
For the first time, we apply this to error analysis by using a Petrov-Galerkin discretization. A some schemes are then implemented: Streamline Upwind PG, Residual Dis-

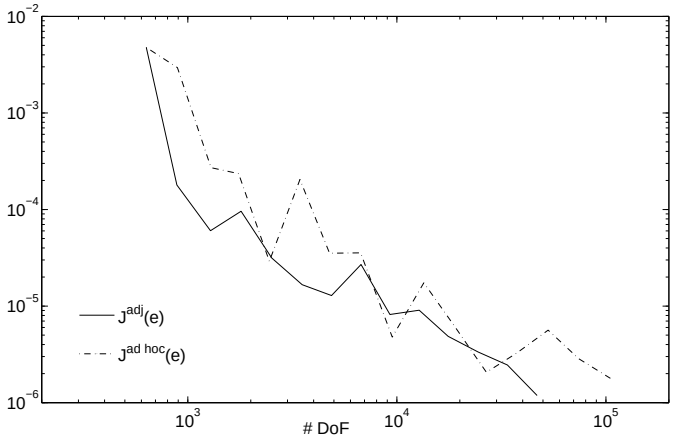


**Figure 5:** Convergence of the target quantity error, $J(e)$

tribution and a bubble scheme. Theory proves that the convergence rate of the target quantity error depends on the scheme chosen. Few linear problems have been employed to verify the behaviour of these schemes, while an hyperbolic problem has been used to test the efficency of the current refinement with respect to the classical residual based estimation. Now, further extensions to non-linear hyperbolic problems are possible.

# A Strong boundary conditions

Strong boundary conditions are realized by considering an appropriate function (sub)space $\mathcal{V}_{h,p,0} \subset \mathcal{V}_{h,p}$ (or $\mathcal{V}_{B,q,0} \subset \mathcal{V}_{B,q}$) which incorportates directly the conditions on the boundary $\Gamma$. Then, the function spaces to search the primal and adjoint solutions that also include homogenous boundary conditions are, respectively,

$$\begin{aligned} \mathcal{V}_{h,p,0} &= \{v : v \in C^0(\Omega), v|_\kappa \in \mathcal{P}_p(\kappa), \forall \kappa \in \mathcal{K},\ Bv = 0 \text{ on } \Gamma\} \\ \mathcal{V}^B_{h,q,0} &= \{v : v|_\kappa \in \mathcal{P}_q(\kappa), \forall \kappa \in \mathcal{K},\ B^*v = 0 \text{ on } \Gamma\} \end{aligned} \tag{35}$$

and so the corresponding bilinear operator is given by

$$\mathcal{B}_0(u_{h,0}, v_b) = (u_{h,0}, L^* v_b)_\Omega + \sum_k (H(u_{h,0}, \boldsymbol{n}), v_B^+)_{\partial\kappa \setminus \Gamma}$$

For the realization of the inhomogeneous inflow boundary conditions, assume that $u_h = u_{h,0} + u_g$ with $u_g \in \mathcal{V}_{h,p}$ and such that $Bu_h = g$ on $\Gamma$; since $Bu_{h,0}\big|_\Gamma = 0$, by definition, then $Bu_g = g$ on $\Gamma$. The same approch is taken for $z_B = z_{B,0} + z_{\hat{\jmath}_\Gamma}$, with $z_{\hat{\jmath}_\Gamma} \in \mathcal{V}_{h,q}$ and where $B^* z_B = \hat{\jmath}_\Gamma$ and $B^* z_{B,0} = 0$ on $\Gamma$ such that $B^* z_{\hat{\jmath}_\Gamma} = \hat{\jmath}_\Gamma$ on $\Gamma$.

# References

[1] P. Hansbo K. Eriksson, D. Estep and C. Johnson. Introduction to adaptive methods for different equations. *Acta Numerica*, pages 105–158, 1995.

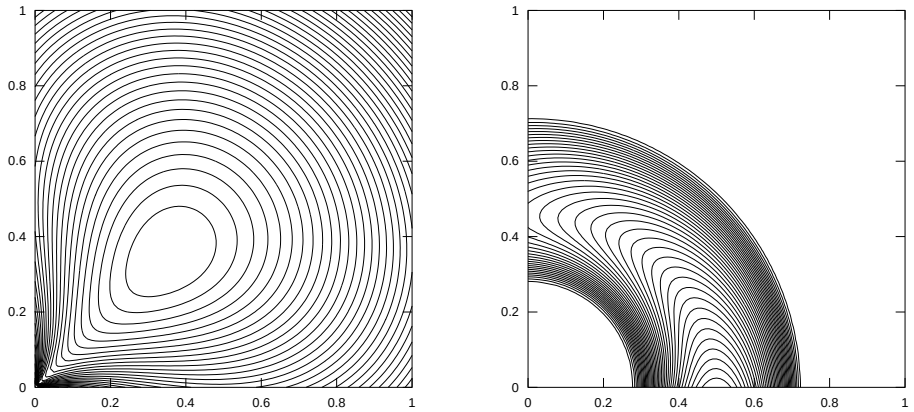


**(a)** **(b)**

**Figure 6:** Analytical solutions circular-reaction problem: (a) primal; (b) adjoint

[2] R. Becker and R. Rannacher. A feed-back approach to error control in finite element methods: basis analysis and examples. *Journal Numerical Mathematics*, 4:237–264, 1996.

[3] R. Becker and R. Rannacher. An optimal control approach to a-posteriori error estimation in finite element methods. *Acta Numerica*, 10:1–102, 2001.

[4] R. Hartmann. *Adaptive Finite Element Methods for the Compressible Euler Equations*. PhD thesis, Universität Heidelberg, 2002.

[5] R. Hartmann. Numerical analysis of higher order discountinuos galerkin finite element methods. In *35th CFD VKI / ADIGMA*, 2008.

[6] T. Barth. *A Posteriori* error estimation and mesh adaptivity for finite volume and finite element methods. Technical report, NASA Ames Research Center, 2002.

# Acknowledgements

Work started during a visit of the first author in Bordeaux, partly funded by the ERC ADDECCO, #226316. MR and RA were partly funded by the ERC ADDECCO, #226316

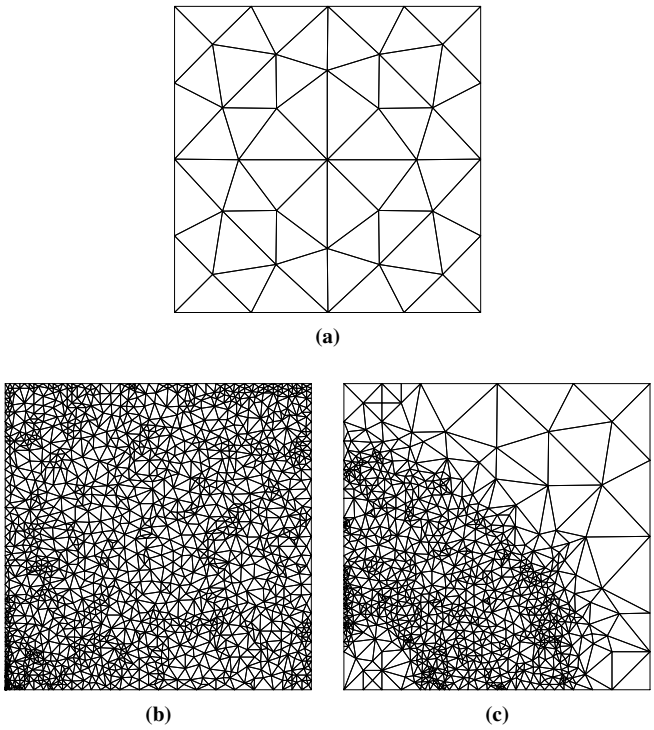


**Figure 7:** Adaptive refinement for the circular-reaction problem (34): (a) Initial mesh; (b) Final mesh generated by the adjoint error estimation; (c) Final mesh generated by the based-residual error estimation

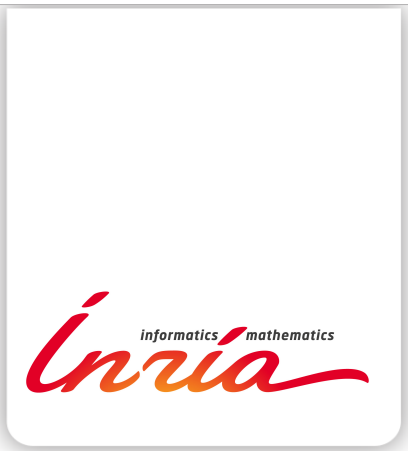


**RESEARCH CENTRE**
**BORDEAUX – SUD-OUEST**

351, Cours de la Libération
Bâtiment A 29
33405 Talence Cedex

Publisher
Inria
Domaine de Voluceau - Rocquencourt
BP 105 - 78153 Le Chesnay Cedex
inria.fr

ISSN 0249-6399